$\Delta\mathcal{N}$ and the stochastic conveyor belt of ultra slow-roll inflation

Tomislav Prokopec
Institute for Theoretical Physics, Spinoza Institute and the Center for Extreme Matter and Emergent Phenomena, Utrecht University, Buys Ballot Building, Princetonplein 5, 3584 CC Utrecht, Netherlands

Gerasimos Rigopoulos
School of Mathematics, Statistics, and Physics, Herschel Building, Newcastle University, Newcastle upon Tyne NE1 7RU, United Kingdom

(Received 17 November 2020; accepted 15 August 2021; published 1 October 2021)

We analyze field fluctuations during an ultra slow-roll phase in the stochastic picture of inflation and the resulting non-Gaussian curvature perturbation, fully including the gravitational backreaction of the field's velocity. By working to leading order in a gradient expansion, we first demonstrate that consistency with the momentum constraint of general relativity prevents the field velocity from having a stochastic source, reflecting the existence of a single scalar dynamical degree of freedom on long wavelengths. We then focus on a completely level potential surface, $V = V_0$, extending from a specified exit point ϕ_e, where slow roll resumes or inflation ends, to $\phi \to +\infty$. We compute the probability distribution in the number of e-folds $\mathcal{N}$ required to reach ϕ_e, which allows for the computation of the curvature perturbation. We find that, if the field's initial velocity is high enough, all points eventually exit through ϕ_e and a finite curvature perturbation is generated. On the contrary, if the initial velocity is low, some points enter an eternally inflating regime despite the existence of ϕ_e. In that case, the probability distribution for $\mathcal{N}$, although normalizable, does not possess finite moments, leading to a divergent curvature perturbation.

DOI: 10.1103/PhysRevD.104.083505

I. INTRODUCTION

The $\Delta\mathcal{N}$ formalism is a very convenient way to compute the curvature perturbation generated during inflation. Its basic tenet is that quantum fluctuations stretched to superhorizon scales introduce randomness in the total number of e-folds at different points in the universe, with this number of e-folds counted from a given initial spatially flat time slice to a given final uniform ϕ time slice. This final time slice is determined by a prescribed condition on the scalar field—for example, that slow roll, and presumably inflation, ends. This difference in the number of e-folds between different spatial points directly gives the scalar curvature perturbation. The idea that a time delay encodes the curvature perturbation induced by the fluctuations of the inflaton goes back to the early days of inflationary cosmology and was already used in some of the pioneering papers on inflationary pertubations [1,2]. The relation of classicalized, super-Hubble modes to a time delay in the dynamics was clearly explained in Ref. [3]. The concept was further formalized and connected to the conserved gauge invariant curvature perturbation in Ref. [4] and later in Refs. [5,6]. More recently, it was reintroduced and elaborated in Refs. [7,8]—see also, e.g., Refs. [9,10].

In the usual slow-roll scenario, the number of e-folds between the prescribed time slices is dominated by the classical/deterministic result, and random perturbations are introduced only as a fluctuation of the initial condition in ϕ, generated when a given mode exits the Hubble radius. In this regime, the evolution of the probability distribution is dominated by the drift term of the Fokker-Planck equation. However, when the potential is very flat, as in the case of ultra slow roll [11–15], and the drift term is small, the slow-roll formula for the curvature perturbation cannot be used anymore, and the e-fold number becomes an essentially stochastic quantity. When asking for the time it takes for the field to reach the prescribed value ϕ_e, we are thus facing a *first-passage time* problem in the stochastically evolving system: Given an initial condition, how many e-folds $\mathcal{N}$ are needed for ϕ_e to be reached? The total number of e-folds becomes a stochastic quantity described by a probability distribution $\varrho(\mathcal{N})$, such that $\varrho(\mathcal{N})d\mathcal{N}$ is the probability that the field will reach ϕ_e for the first time within the interval $[\mathcal{N}, \mathcal{N} + d\mathcal{N})$ of e-folds [16–21]. As alluded to above, one can define the first passage with respect to any desirable condition labeled by ϕ_e and defined by a constant field hypersurface where $\phi = \phi_e$, such as inflation ending or the commencement of another distinct phase.

The curvature perturbation generated during a phase of ultra slow roll (USR) has attracted considerable attention recently [22–29] due to the possibility that it leads to an enhanced curvature perturbation and a related enhanced primordial black hole production—see Ref. [30] for a recent review on cosmological implications of primordial black holes. In this work we revisit the problem, taking the scalar sector of gravity fully into account. We place the computation within the framework of a long-wavelength (leading gradient) approximation to the equations of general relativity for an inhomogeneous universe: we retain full nonlinearities but drop terms that are second order in spatial gradients, and properly take into account the field's velocity and the corresponding gravitational backreaction. Quantum fluctuations are then consistently included as a random forcing of the dynamical equation of the scalar field, a well-established approximation for IR quantum fields in inflationary spacetimes [16,31–36]. We find that imposing the $0i$ Einstein equation, the GR momentum constraint, leads to the field ϕ being the only dynamical stochastic variable. The field's velocity is constrained and does not obey an independent equation involving different stochastic kicks at different spatial points, unlike what a naive "separate universe" argument would imply. This is a nonlinear generalization of the linear perturbation theory result for $k/aH \to 0$ [4,37].

We apply the formalism to a simple problem: the curvature fluctuation generated in an extreme version of USR where the field is injected at some point $\phi_{\rm in}$ with velocity $\Pi_{\rm in}$ on a totally flat potential $V = V_0$. We find two separate regimes, depending on the distance from $\phi_{\rm in}$ to the exit point $\phi_{\rm e}$ and the initial velocity. If this distance is larger than the length of the classical trajectory, corresponding to a low injection velocity $\Pi_{\rm in}$, the field experiences what we call the *stochastic conveyor belt model* for USR: in some parts of the universe, the initial velocity is forgotten and the field explores the infinite semiline $\phi \to \infty$, never fully reaching $\phi_{\rm e}$. The resulting probability distribution for the total number of e-folds $\mathcal{N}$ is normalizable but does not have finite moments, leading to the infinite inflation observed in Refs. [38,39]. However, if the distance is smaller than the length of the classical trajectory, corresponding to a high injection velocity $\Pi_{\rm in}$, graceful exit does occur, and inflation eventually terminates in all points of the universe. The curvature perturbation is then finite and is described by a highly non-Gaussian probability distribution that we compute.

Obviously, the infinite inflation regime will not be reached in realistic single-field models, where USR takes place only on a finite portion of the potential. This paper then serves an expository function for the developed techniques, involving mainly the use of the Hamilton-Jacobi equation for inflationary evolution, the consistent inclusion of stochastic fluctuations, and the description of the stochastic conveyor belt mechanism. These techniques will be used to analyze more realistic USR potentials in a forthcoming publication [40].

II. LONG-WAVELENGTH SCALAR PERTURBATIONS

We start by recalling the long-wavelength approach of Ref. [4] (see also Ref. [41]), which will take us to the starting point of our stochastic analysis. Considering the metric in its ADM parametrization,

$$g_{00} = -N^2 + \gamma^{ij}N_iN_j, \qquad g_{0i} = N_i, \qquad g_{ij} = \gamma_{ij}, \tag{1}$$

where N and N_i are the lapse function and shift vector, respectively, the Einstein equations for gravity plus a single scalar field ϕ give the GR energy and momentum constraints (00 and $0i$ Einstein equations)

$$\bar{K}_{ij}\bar{K}^{ij} - \frac{2}{3}K^2 - {}^{(3)}R + 16\pi G\varepsilon = 0, \tag{2}$$

$$\bar{K}^j_{i|j} - \frac{2}{3}K_{|i} + 8\pi G\Pi\phi_{|i} = 0, \tag{3}$$

the dynamical equations for the extrinsic curvature tensor of the 3-slices $K_{ij} = \bar{K}_{ij} + \frac{1}{3}K\gamma_{ij}$ are

$$\frac{\partial K}{\partial t} - N^iK_{|i} = -N^{|i}{}_{|i} + N\left[\frac{3}{4}\bar{K}_{ij}\bar{K}^{ij} + \frac{1}{2}K^2 + \frac{1}{4}{}^{(3)}R + 4\pi GS\right], \tag{4}$$

$$\frac{\partial \bar{K}^i{}_k}{\partial t} + N^i{}_{|l}\bar{K}^l_k - N^l{}_{|k}\bar{K}^i_l - N^l\bar{K}^i_{k|l} = -N^{|i}{}_{|k} + \frac{1}{3}N^{|l}{}_{|l}\delta^i_k + N\left[K\bar{K}^i_k + {}^{(3)}\bar{R}^i_k - 8\pi G\bar{S}^i_k\right] \tag{5}$$

(stemming from the ij Einstein equation), and the equation of motion for the scalar field is

$$\frac{1}{N}\left(\frac{\partial \Pi}{\partial t} - N^i\Pi_{|i}\right) - K\Pi - \frac{1}{N}N_{|i}\phi^{|i} - \phi_{|i}\phi^{|i} + \frac{dV}{d\phi} = 0. \tag{6}$$

In the above, the field momentum Π is defined as

$$\Pi = \frac{1}{N}\left(\frac{\partial\phi}{\partial t} - N^i\phi_{|i}\right), \tag{7}$$

the extrinsic curvature 3-tensor is

$$K_{ij} = -\frac{1}{2N}\left(\frac{\partial\gamma_{ij}}{\partial t} - N_{i|j} - N_{j|i}\right), \tag{8}$$

and the scalar's energy density and the stress tensor on the 3-slices read

$$\varepsilon = \frac{1}{2}(\Pi^2 + \phi_{|i}\phi^{|i}) + V(\phi) \tag{9}$$

and

$$S_{ij} = \phi_{|i}\phi_{|j} + \gamma_{ij}\left(\frac{1}{2}\Pi^2 - \frac{1}{2}\phi_{|i}\phi^{|i} - V(\phi)\right). \quad (10)$$

A vertical bar denotes a covariant derivative with respect to the 3-metric γ_{ij}, which is also used to raise or lower spatial indices.

The approximation we use to study the nonlinear long-wavelength configurations relevant for inflation is to only keep terms containing the leading order in spatial derivatives. This is underpinned by the expectation that on scales $aL > H^{-1}$ the dynamics is dominated by time derivatives such that for any quantity Q, the inequality $\|e^{-\alpha}\nabla Q\| < |\partial_t Q|$ will be true, where $\dot{\alpha}$ denotes the local expansion rate [see Eqs. (15) and (17) below], a statement that in inflation is expected to eventually hold for all scales of interest. Furthermore, to simplify the equations, we choose to consider coordinate systems constructed such that $N_i = 0$. This gauge choice fixes three gauge degrees of freedom, leaving one gauge function unfixed; its elimination can be achieved—e.g., by further choosing a specific form for the lapse function N. Under these assumptions, we get from Eq. (5) that the traceless part of the extrinsic curvature evolves according to

$$\frac{\partial \bar{K}^i{}_k}{\partial t} = NK\bar{K}^i_k. \quad (11)$$

The 3-metric can be further decomposed as

$$\gamma_{ij} = e^{2\alpha}h_{ij}, \quad (12)$$

where $\mathrm{Det}\, h_{ij} = 1$ and therefore $h^{ij}\frac{\partial}{\partial t}h_{ij} = 0$. We then have

$$K = -3\dot{\alpha} \equiv -3\frac{1}{N}\frac{\partial \alpha}{\partial t}, \quad (13)$$

from which we directly obtain

$$\bar{K}^i{}_j = C^i{}_j(\mathbf{x})e^{-3\alpha}, \qquad \mathrm{Tr}[C^i{}_j(\mathbf{x})] = 0. \quad (14)$$

Since during inflation $\alpha(t,\mathbf{x})$ represents the local generalization of the number of e-folds, it grows approximately linearly in time, and we can take it as a proxy for *time* in inflation. Therefore, Eq. (14) tells us that the anisotropic expansion rate $\bar{K}^i{}_j$—which is the nonlinear generalization of the canonical momentum associated with gravitational waves—declines extremely rapidly (exponentially fast) during inflation. We are thus dynamically led to $\bar{K}^i{}_j = 0$, and the most general 3-metric on long wavelengths can be written as

$$\gamma_{ij}(t,\mathbf{x}) = e^{2\alpha(t,\mathbf{x})}h_{ij}(\mathbf{x}), \quad (15)$$

with the long-wavelength spacetime metric taking the form

$$ds^2 = -N^2(t,\mathbf{x})dt^2 + e^{2\alpha(t,\mathbf{x})}h_{ij}(\mathbf{x})dx^i dx^j, \quad (16)$$

and the 3-tensor h_{ij} is not dynamical in this approximation, at least classically. Furthermore, we restrict the lapse function $N(t,\mathbf{x})$ to vary slowly enough in space that its spatial gradients can be neglected. Later on, we will consider scalar quantum fluctuations, and the accompanying tensor fluctuations would provide h_{ij} with a stochastic source from subhorizon tensor modes entering the long-wavelength sector, and with an amplitude set by the uncertainty principle. In this work, we focus on the dynamics of the scalar sector of gravity, leaving that of the stochastic evolution of the tensor sector for future study.

Defining the local expansion rate as

$$H(t,\mathbf{x}) \equiv \frac{1}{N}\frac{\partial \alpha}{\partial t}, \quad (17)$$

we are led to a set of long-wavelength equations for the spatially dependent field $\phi(t,\mathbf{x})$ and expansion rate $H(t,\mathbf{x})$ comprising the two GR constraints: the energy [Eq. (2)] and momentum [Eq. (3)] constraints (from now on, we set $8\pi G = 1$)[1]:

$$H^2 = \frac{1}{3}\left(\frac{1}{2}\Pi^2 + V(\phi)\right) \quad (18)$$

and

$$\partial_i H = -\frac{1}{2}\Pi\partial_i\phi, \quad (19)$$

the evolution of the expansion rate [Eq. (4)],

$$\frac{1}{N}\frac{\partial H}{\partial t} = -\frac{1}{2}\Pi^2, \quad (20)$$

as well as the dynamical equations for the scalar field [Eqs. (6) and (7)],

$$\Pi = \frac{1}{N}\frac{\partial \phi}{\partial t}, \quad (21)$$

$$\frac{1}{N}\frac{\partial \Pi}{\partial t} + 3H\Pi + \frac{dV}{d\phi} = 0. \quad (22)$$

Equations (18), (20), (21) and (22) are formally the same as those of homogeneous cosmology but are valid at each spatial point with *a priori* different values of the initial

[1]The Newton constant $8\pi G = 1/M_{\mathrm{P}}^2$ can always be recovered in the equations by noting the canonical dimension of various quantities: $[H] = 1$, $[\phi] = 1$, $[8\pi G] = -2$, $[\Pi] = 2$, $[V(\phi)] = 4$, $[h_{ij}] = 0$.

conditions for ϕ and Π. This is what is sometimes referred to as the "*separate universe evolution*." However, not all spatially inhomogeneous initial conditions are allowed on long wavelengths, as they must also satisfy the momentum constraint [Eq. (19)]. As we will see, this restricts the possibility of assigning Π independently of the initial value of ϕ. Indeed, for the constraint (19) to be respected, the local expansion rate H must depend on the spatial position only through its dependence on the spatially varying ϕ,

$$H(t,\mathbf{x}) = H(\phi(t,\mathbf{x}),t), \tag{23}$$

and the field momentum must be given by

$$\Pi = -2\frac{\partial H}{\partial \phi}. \tag{24}$$

Taking the time derivative of Eq. (23) and comparing with Eq. (20), we immediately find that

$$\left(\frac{\partial H}{\partial t}\right)_{\phi} = 0, \tag{25}$$

showing that the total spatiotemporal dependence of the expansion rate is solely determined through its dependence on $\phi(t,\mathbf{x})$:

$$H = H(\phi(t,\mathbf{x})), \tag{26}$$

and the field momentum is therefore given by

$$\Pi = -2\frac{dH}{d\phi}. \tag{27}$$

Hence, Π is evidently also a function of ϕ alone, $\Pi = \Pi(\phi(t,\mathbf{x}))$, with no explicit temporal or spatial dependence.

When Eq. (27) is inserted into the local energy constraint [Eq. (19)], it gives the *Hamilton-Jacobi equation* for the function $H(\phi)$:

$$\left(\frac{dH}{d\phi}\right)^2 = \frac{3}{2}H^2 - \frac{1}{2}V(\phi). \tag{28}$$

Since Eq. (28) is a first-order differential equation, it admits a family of solutions of the form $H(\phi,\mathcal{C})$, with different solutions parametrized by an arbitrary constant $\mathcal{C}$. A solution $H = H(\phi,\mathcal{C})$ to Eq. (28), along with

$$\frac{d\phi}{dt} = -2N\frac{dH}{d\phi}, \tag{29}$$

provides a *complete description* and the inhomogeneous long-wavelegth scalar field configuration ϕ.[2] The corresponding long-wavelength metric [Eq. (16)] can then determined via

$$\frac{1}{N}\frac{\partial\alpha}{\partial t} = H(\phi). \tag{30}$$

It should be pointed out that by taking a ϕ derivative of Eq. (18), one can verify that the long-wavelength field indeed obeys

$$\frac{1}{N}\frac{\partial}{\partial t}\left(\frac{1}{N}\frac{\partial\phi}{\partial t}\right) + 3H\frac{1}{N}\frac{\partial\phi}{\partial t} + \frac{dV}{d\phi} = 0 \tag{31}$$

as expected. Although Eqs. (28)–(30) are identical to those of homogeneous cosmology, including Eq. (31), which is implied by them, the momentum constraint [Eq. (19)] imposes that there is no freedom to choose initial values for Π independently at each spatial point. Let us see why: If Eq. (28) is considered without reference to Eq. (19), a naive separate universe picture would imply that $\mathcal{C} = \mathcal{C}(\vec{x})$—i.e., for every point $\vec{x}$ on the initial hypersurface, there would be a separate integration constant $\mathcal{C}(\vec{x})$. This simply encodes the freedom to choose the initial field momentum at that point independently of ϕ. However, a spatially inhomogeneous $\mathcal{C}(\vec{x})$ further leads to

$$\nabla H = (\partial_{\mathcal{C}}H)\nabla\mathcal{C} + (\partial_{\phi}H)\nabla\phi \neq -\frac{1}{2}\Pi\nabla\phi. \tag{32}$$

Therefore, as long as $\partial_{\mathcal{C}}H \neq 0$, it follows that $\nabla\mathcal{C} = 0$; otherwise, the momentum constraint [Eq. (19)] would be violated. This restricts $\mathcal{C}$ to be a global constant, meaning that the momentum Π cannot be chosen arbitrarily at each point, but instead, all spatial points must be placed along one and the same integral curve of Eq. (28).

The restriction $\nabla\mathcal{C} = 0$ is a direct consequence of the momentum constraint. However, it would not apply when integral curves of $H(\phi,\mathcal{C})$ exist for which $\partial_{\mathcal{C}}H = 0$. In this case, setting $\nabla\mathcal{C} \neq 0$ would not violate the momentum constraint, since a spatially varying value of $\mathcal{C}$ does not change the value of H at different spatial points. Such integral curves are attractors of the long-wavelength system, as one can see by taking a derivative of Eq. (28) with respect to $\mathcal{C}$, which leads to [4,41]

$$\frac{\partial H}{\partial\mathcal{C}} \propto a^{-3}. \tag{33}$$

[2]Equation (28), often referred to as the Hamilton-Jacobi equation in the literature, has been used in Refs. [42,43] to study an alternative parametrization of possible homogeneous inflationary cosmologies, including USR [12,44]. We stress that in the present, long-wavelength context, it describes an *inhomogeneous* universe as well, as originally demonstrated in Ref. [4].

This is equivalent to the decay of the second solution to Eq. (31) and, as was already pointed out in Ref. [9], if this decaying mode is neglected, the momentum constraint places no further restriction on the long-wavelength configuration; this is the case, for example, in slow-roll inflation. In the case of motion on a constant potential examined in this work, the decaying mode [Eq. (33)] expresses the approach to a static field and de Sitter spacetime—see Eq. (38), where the constant ϕ_0 in that formula plays the role of the general constant $\mathcal{C}$ discussed here. Including this decaying mode is therefore crucial in studying the slide and slowing down of the field on the constant potential. More generally, the Hamilton-Jacobi treatment adopted here allows the $\Delta\mathcal{N}$ formalism to be made fully and *a priori* consistent with the momentum constraint and include the decaying mode, which is essential in studying ultra slow roll.

We can conclude that on sufficiently large scales, at which subleading spatial gradient terms can be neglected, the dynamics of the inhomogeneous configuration can be described solely in terms of ϕ, while the momentum, when it contributes to the expansion rate, cannot be arbitrarily chosen at different spatial points. The would-be inhomogeneous degree of freedom is killed by the momentum constraint [Eq. (19)] on long wavelengths, which patches different spatial points together. Physically, that means that on large scales, there is a decaying inhomogeneous mode which is necessarily suppressed by spatial derivatives, and hence negligible in the leading gradient expansion. We stress that this conclusion goes beyond slow roll and is completely general, relying only on the long-wavelength approximation. Note that slow roll trivially satisfies the momentum constraint and is an attractor in which any dependence of H on $\mathcal{C}$ is altogether suppressed exponentially. The absence of a second dynamical inhomogeneous mode is unique to single-scalar inflationary models. For a recent study on how the inflaton canonical momentum can be excited during inflation through its coupling to a light spectator scalar field, see Ref. [45].

Before closing this section, we note that Eqs. (28)–(30) and the corresponding metric (16) are valid for *any* choice of time hypersurfaces (any choice of N), as long as the corresponding spatial coordinate worldlines are constructed orthogonally to the time slices, keeping $N_i = 0$, and if all terms that are second order in spatial gradients are dropped; see Ref. [4]. For the reader's convenience, we recall the demonstration of this fact in Appendix A.

III. HAMILTON-JACOBI SOLUTION IN ULTRA SLOW ROLL

We now apply the above analysis to our extremal USR scenario, where the field moves along a very flat and level part of the potential where $V(\phi) \simeq V_0$. Equation (28) then reads

$$\left(\frac{dH}{d\phi}\right)^2 = \frac{3}{2}H^2 - \frac{1}{2}V_0. \tag{34}$$

Taking a derivative with respect to ϕ gives

$$\frac{dH}{d\phi}\left(\frac{d^2H}{d\phi^2} - \frac{3}{2}H\right) = 0, \tag{35}$$

and the general solution can be written as

$$H(\phi) = H_0 = \sqrt{\frac{V_0}{3}}, \quad \text{or} \quad H(\phi) = A\mathrm{e}^{-\sqrt{\frac{3}{2}}\phi} + B\mathrm{e}^{\sqrt{\frac{3}{2}}\phi}, \tag{36}$$

where $AB = \frac{V_0}{12}$. The constraints on the integration constants H_0 and AB are obtained by inserting the general solutions of Eq. (35) into the original Hamilton-Jacobi equation (34). It is convenient to redefine A and B as

$$A = \frac{H_0}{2}\mathcal{C} = \frac{H_0}{2}\mathrm{e}^{\sqrt{\frac{3}{2}}\phi_0}, \quad B = \frac{H_0}{2}\mathcal{C}^{-1} = \frac{H_0}{2}\mathrm{e}^{-\sqrt{\frac{3}{2}}\phi_0}, \tag{37}$$

where $\mathcal{C}$ and ϕ_0 are global constants. With these definitions in mind, the second solution in Eq. (36) becomes

$$\begin{aligned} H(\phi) &= \frac{H_0}{2}\left(\mathcal{C}\mathrm{e}^{-\sqrt{\frac{3}{2}}\phi} + \mathcal{C}^{-1}\mathrm{e}^{\sqrt{\frac{3}{2}}\phi}\right) \\ &= H_0 \cosh\left(\sqrt{\frac{3}{2}}(\phi - \phi_0)\right), \end{aligned} \tag{38}$$

where we have replaced $\mathcal{C}$ with $\phi_0 = \sqrt{\frac{2}{3}}\ln(\mathcal{C})$. The corresponding momentum (velocity) is then taken from Eq. (24):

$$\Pi = 0, \quad \text{or} \quad \Pi = -\sqrt{6}H_0 \sinh\left(\sqrt{\frac{3}{2}}(\phi - \phi_0)\right). \tag{39}$$

The number of e-foldings α, from Eq. (17) and using the solution for $H(\phi)$ Eq. (38), becomes

$$\alpha = \int HN dt = -\frac{1}{6}\ln\left[\sinh^2\left(\sqrt{\frac{3}{2}}(\phi - \phi_0)\right)\right]. \tag{40}$$

The above formulas completely describe the classical field evolution along a flat potential $V = V_0$, including the gravitational backreaction of a nonzero field velocity. However, they require some clarification with regard to the exact dynamics they describe. We see that if the field starts off with a finite velocity, it evolves asymptotically towards ϕ_0, which it reaches only after an infinite amount of e-folds. The precise value of ϕ_0 depends on the initial velocity imparted on ϕ as well as its sign: If $\Pi(\phi_{\rm in}) > 0$, then $\phi_0 > \phi(t)$, and ϕ moves asymptotically to the right towards ϕ_0. If $\Pi(\phi_{\rm in}) < 0$, then $\phi_0 < \phi(t)$, and ϕ moves asymptotically to the left towards ϕ_0. Of course, if $\Pi(\phi_{\rm in}) = 0$, then the field remains static, and these are degenerate "trajectories," where $\Pi = 0$ and $H = H_0$ always. Note that they represent distinct solutions of Eq. (28), and the field does not transition from a $\Pi \neq 0$ to a $\Pi = 0$ state during its classical evolution, nor does its velocity change sign. The constant ϕ_0 is the asymptotic end point of each classical trajectory, and it parametrizes different integral curves of the HJ equation (28); it is identified with the constant $\mathcal{C}$ of the general discussion in Sec. II. Note that $\partial_{\phi_0} H|_{\phi=\phi_0} = 0$, and therefore a static field can become inhomogeneous without violating the momentum constraint. Figure 1 summarizes the different solutions. We therefore see that on long wavelengths and for a flat level potential,

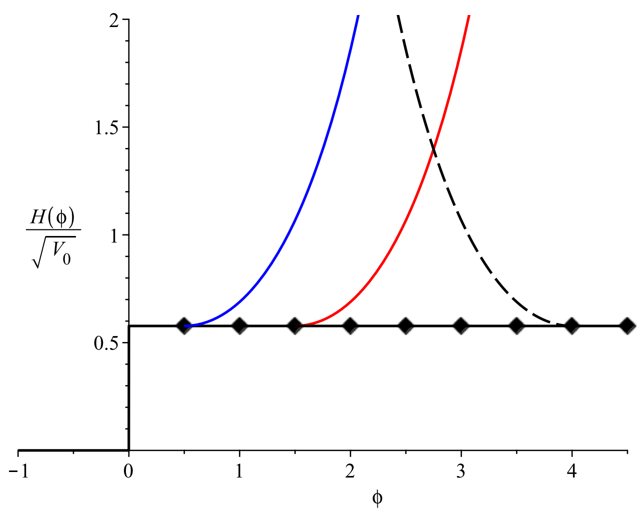

FIG. 1. The conveyor belt of stochastic ultra slow roll: Solutions of the HJ equation of motion on a flat potential $V(\phi) = V_0$ are plotted. Inflation ends at $\phi = 0$ in this figure. The blue and red curves are HJ solutions for fields moving to the left (negative initial velocity), while the dashed curve shows a trajectory that started off with positive initial velocity. These evolving trajectories reach the $H_0^2 = V_0/3$ surface only asymptotically after an infinite number of e-folds. Alternatively, the field can remain stationary at some value of ϕ on one of the $H_0^2 = V_0/3$ points—a sample of them are denoted in the figure by diamonds. Classically, the field does not transition from an evolving state to a stationary state, and therefore the classical phase space is partitioned into these two types of trajectories. Stochastic fluctuations disintegrate this partition: the field can start along one of the HJ trajectories, but it is now possible to cross the asymptotic end point due to a stochastic jump. This end point acts as a bifurcation point for the quantum phase space, beyond which the field simply diffuses along the $H^2 = V_0/3$ surface. The GR momentum constraint is still respected, since $\Pi = 0$ there. The system thus resembles a jiggly conveyor belt where an initial HJ trajectory feeds into a de Sitter stage with successive unimpeded diffusion.

(1) An *evolving* ($\Pi \neq 0$) long-wavelength field configuration always tends at asymptotically late times to the *same* field value at all spatial points: $\phi(t, \mathbf{x}) \to \phi_0$.
(2) An arbitrary *inhomogeneous* field configuration is only allowed for a *static* field, since $\partial_{\phi_0} H|_{\phi=\phi_0} = 0$ in this case. This is a nonlinear version of the growing mode of linearized pertubations.

As emphasized above, these represent two different solutions, which classically do not evolve into each other. In the following section, we discuss how this picture changes when quantum effects are included.

IV. STOCHASTIC EVOLUTION: THE CONVEYOR BELT OF ULTRA SLOW ROLL

Let us now incorporate a stochastic element in the evolution, modeling as usual quantum fluctuations stretched to long wavelengths. We do not need to specify the amplitude of the noise terms at this point, so we keep them general for this discussion. Generically, any stochastic "add-on" to the dynamics, regardless of the microscopic origin of the extra noise terms, can be thought of as adding an extra stochastic "kick" to the classical drift determined by the dynamical equations. Suppose we introduce noise in both the field and its momentum: in a discretized form of the time evolution, their values would be updated after a time step Δt as

$$\Delta\phi = -2\frac{\partial H}{\partial \phi} N\Delta t + \xi_\phi N\Delta t,$$
$$\langle \xi_\phi(t)\xi_\phi(t')\rangle = \mathcal{A}\delta(t-t'), \tag{41}$$

$$\Delta\Pi = -3H\Pi N\Delta t + \xi_\Pi N\Delta t,$$
$$\langle \xi_\Pi(t)\xi_\Pi(t')\rangle = \mathcal{B}\delta(t-t'). \tag{42}$$

To be consistent with the constraints, H should be a solution to the Hamilton-Jacobi equation. For the case we are considering, it is given by Eq. (38) with either $\phi > \phi_0$ or $\phi < \phi_0$ depending on the sign of the velocity—see Fig. 1.

The energy and momentum constraints are not dynamical equations, and therefore they are not to be accompanied by some form of an extra stochastic force. As is well known, the constraints are preserved by the classical dynamical evolution, and any consistent stochastic extension of the dynamics should also preserve them while the stochastic kicks are incorporated—the stochastically updated field and momentum should respect them too. We can achieve this by elevating the constants appearing in the solution of the HJ equation, whose values parametrize different possible velocities for fixed field values, to stochastic variables. Let us now see how this can be done in our case.

The constant ϕ_0 in Eq. (39), characterizing different HJ solutions, can be linked to the velocity, since we can write

$$\phi_0 = \phi - \sqrt{\frac{2}{3}}\text{arc sinh}\left(-\frac{\Pi}{\sqrt{2}V_0^{1/2}}\right), \tag{43}$$

and the choice of Π for fixed ϕ is reflected in ϕ_0, which also defines the breadth of field values covered by motion on the flat potential given the initial Π of the field. If many possible initial conditions for Π are contemplated, then ϕ_0 defines the different asymptotic resting points corresponding to different initial momenta $\Pi_{\rm in}$ for a given initial value of ϕ. A stochastic change in Π at fixed ϕ would correspond to the field changing the HJ curve along which it evolves, and this can be accommodated by promoting ϕ_0 to a stochastic variable which would change according to[3]

$$\Delta\phi_0 = \Delta\phi + \frac{\Delta\Pi}{3H} + \frac{1}{18H^3}\frac{\partial H}{\partial\phi}\Delta\Pi^2, \tag{44}$$

leading to

$$\Delta\phi_0 = \frac{N\mathcal{B}}{18H^3}\frac{\partial H}{\partial\phi}N\Delta t + \left(\frac{1}{3H}\xi_\Pi + \xi_\phi\right)N\Delta t. \tag{45}$$

At face value, this provides a stochastic equation for ϕ_0 which would now take different values at different spatial points. However, as we stressed above, unless $\frac{\partial H}{\partial\phi_0} = -\frac{\partial H}{\partial\phi} = \frac{\Pi}{2} = 0$, ϕ_0 should only take a global value if the momentum constraint is to be respected. This cannot be accommodated in Eq. (45), since, for any choice of ξ_ϕ and ξ_Π, ϕ_0 necessarily develops inhomogeneities. Hence, although one could *a priori* allow for stochastic changes in the velocity through stochastically jumping between different HJ trajectories on top of the stochastic ϕ displacement, the momentum constraint prevents that if $\Pi \neq 0$.

We are thus led to conclude that as long as $\Pi \neq 0$, the whole long-wavelegth universe can only be located on different points of a single HJ trajectory with the following stochastic equation:

$$\Delta\phi = -2\frac{\partial H(\phi,\phi_0)}{\partial\phi}N\Delta t + \xi_\phi N\Delta t,$$
$$\langle\xi_\phi(t)\xi_\phi(t')\rangle = \mathcal{A}\delta(t-t'), \tag{46}$$

with either $\phi > \phi_0$ or $\phi < \phi_0$, depending on the fixed sign of the momentum. Once stochastic evolution takes the field past ϕ_0, memory of the initial velocity is lost, and it simply diffuses by a free random walk on the flat potential surface V_0, obeying

$$\Delta\phi = \xi_\phi(t,\mathbf{x})N\Delta t, \qquad \langle\xi_\phi(t)\xi_\phi(t')\rangle = \mathcal{A}\delta(t-t'). \tag{47}$$

In this regime, the field does jump between different HJ trajectories—i.e., different points on the $H = H_0$ surface. This is now allowed, as these degenerate solutions are characterized by $\partial_{\phi_0}H|_{\phi=\phi_0} = \Pi(\phi_0) = 0$. Hence, the momentum constraint is not violated by the universe occupying different solutions at different spatial points and stochastically jumping between them, becoming a collection of classically static field values that carry no extra energy.

Note that the quantum fluctuations have a remarkable effect. The classical phase space, consisting of the set of trajectories that solve the HJ equation (28) and which are shown in Fig. 1, is split into (i) regular (nondegenerate, HJ) trajectories, which are characterized by an initial momentum $\Pi_{\rm in}$, the corresponding field value, $\phi_{\rm in} = \phi(\Pi_{\rm in})$, and end at $\phi_0 = \phi_0(\Pi_{\rm in})$, at which $\Pi = 0$; and (ii) degenerate trajectories characterized by $\Pi_{\rm in} = 0$ and an arbitrary field value ϕ_0. The quantum phase space is very different, however. A typical quantum/stochastic trajectory consists of a classical HJ branch $\Pi_{\rm in}$, which ends at $\phi_0 = \phi(\Pi_{\rm in})$, supplemented by the set of all degenerate trajectories ($\Pi = 0$, $\phi \in \mathbb{R}$). The point $\phi_0 = \phi(\Pi_{\rm in})$ is a bifurcation point, at which the quantum trajectory splits into two branches: $\phi > \phi_0$ and $\phi < \phi_0$, see Fig. 1. This quantum phase space picture resembles a conveyor belt for the quantum field which starts at a point on one of the HJ branches, diffuses downwards towards the bifurcation point at ϕ_0, and then continues diffusing along the set of points shown as the horizontal line $\Pi = 0$, $H = H_0 \equiv \sqrt{V_0/3}$ in Fig. 1.

Despite field fluctuations being generated, the above picture does not carry with it a well-defined curvature perturbation. A corresponding curvature perturbation emerges only when an exit point $\phi_{\rm e}$ is specified, where either inflation ends or another inflationary era follows by exiting the region where $V(\phi) = V_0$. If $\phi_{\rm e}$ lies outside the HJ branch, we are faced with the stochastic conveyor belt and a double first-passage-time problem: first, to transition from a $\Pi \neq 0$ solution onto the $H = H_0$ surface (as nonstochastic evolution does not allow this), and second, to exit the $H = H_0$ region by reaching $\phi_{\rm e}$. If $\phi_{\rm e}$ is reached within the HJ branch, we have a standard first-passage-time problem, and the conveyor is not operational. We analyze these cases in Secs. V and VI, respectively.

V. THE CASE $\phi_{\rm e} < \phi_0$: USR WITHOUT GRACEFUL EXIT

As we demonstrated above, the gravitationally consistent inclusion of velocity to the problem of diffusion on a flat

[3]Note that we are using Itô's calculus here [46,47], and we therefore keep $\Delta\Pi^2$ terms to follow changes to order Δt. Other choices are possible along with corresponding calculi, and the results are invariant, since $\mathcal{A}$ and $\mathcal{B}$ are independent of ϕ.

potential leads naturally to a two-stage process when $\phi_e < \phi_0$: (i) All spatial points diffuse along a single branch of the HJ solution until ϕ_0 is crossed, and then (ii) each point that has crossed ϕ_0 diffuses independently along the level V_0 potential. We therefore need to construct a first-passage-time probability distribution for the first stage, and for that we require the kernel (to which we shall also refer to as the propagator) with *exit* boundary conditions at ϕ_0, achieved by setting $P_{\rm HJ}(\phi_0, \alpha) = 0$ [48]. The probability current at that point then injects probability for the second stage of the diffusion—one can thus think of the HJ branch as a "conveyor belt" feeding the second diffusive process at a single point ϕ_0.

The stochastic equation describing the IR field dynamics reads

$$d\phi = -2\frac{\partial H}{\partial \phi} d\tau + \xi_\phi d\tau, \tag{48}$$

where ξ_ϕ is the noise generated by the flow of modes between the UV and IR sectors of the theory. When treated perturbatively, due to an effectively time-dependent cutoff, the leading-order contribution occurs at the tree level [16], and on super-Hubble scales the noise is, to a good approximation, of Markovian type:

$$\langle \xi_\phi(\tau)\xi_\phi(\tau')\rangle = \mathcal{A}\delta(\tau - \tau'), \tag{49}$$

where $\tau = \int^t N(t, \vec{x}) dt'$ denotes a reparametrization-invariant time. The coupling between the ultraviolet and long-wavelength modes can then be approximated by its tree-level expression,

$$\mathcal{A} = \frac{(\sigma a H)^3}{2\pi^2}(1-\epsilon)H|\phi(\tau, k)|^2_{k=\sigma a H}[1 + \mathcal{O}(\kappa^2 H^2)], \tag{50}$$

where $\kappa^2 = 16\pi G$ is the loop-counting parameter of quantum gravity and σ sets the highest (ultraviolet cutoff) energy scale of the long-wavelength theory. For example, when $\sigma = 1$, the highest scale (smallest wavelength) is the Hubble scale; when $\sigma \ll 1$, the highest scale is much smaller than the Hubble scale (or equivalently, a wavelength much longer than H^{-1}). Since there can be no secular enhancement in the loop corrections in Eq. (50), the loop suppression factor, $\kappa^2 H^2 \lesssim 10^{-12}$ represents a fair estimate of the accuracy of the stochastic approximation scheme developed in this work. In order to estimate the noise amplitude [Eq. (50)], in what follows, we work in the approximation $\epsilon \approx 0$ and set $\sigma \ll 1$, in which case $|\phi(\tau, k)|^2 \simeq H_0^2/(2k^3)$, and the noise amplitude simplifies to

$$\mathcal{A} \approx \frac{H_0^3}{4\pi^2} \tag{51}$$

which is the approximation we use below. Rigorous proof that Starobinsky's stochastic inflation [16] reproduces the correct infrared dynamics on de Sitter can be found in Refs. [31–36] for interacting scalar field theories and in Ref. [49] for quantum scalar electrodynamics. These works demonstrate that stochastic inflation not only reproduces the leading infrared logarithms at each order in perturbation theory, but (when summed up) they also reveal what happens at late times in the deep nonperturbative regime when the large logarithms overwhelm small coupling constants, a point first made in Ref. [50]. To directly compute the curvature perturbation, we use the number of e-folds α as the time variable.[4] This is, in fact, required for consistency with standard cosmological pertubation theory—see, e.g., Ref. [21]. We therefore have the following branches of the evolution:

HJ branch: The Langevin equation on the HJ branch is

$$\frac{d\phi}{d\alpha} = -2\frac{\partial \ln H(\phi, \phi_0)}{\partial \phi} + \frac{H(\phi, \phi_0)}{2\pi}\xi(\alpha), \tag{52}$$

with

$$\langle \xi(\alpha)\xi(\alpha')\rangle = \delta(\alpha - \alpha') \tag{53}$$

and an absorbing boundary condition at $\phi = \phi_0$. $H(\phi, \phi_0)$ is the solution to the HJ equation, with ϕ_0 determined by the initial velocity of the field. When expressed as a Fokker-Planck equation, this implies that the probability density $P_{\rm HJ}(\phi, \alpha)$ on the HJ branch obeys

$$\frac{\partial P_{\rm HJ}}{\partial \alpha} = -\frac{\partial}{\partial \phi}\left(-2\frac{\partial \ln H}{\partial \phi}P_{\rm HJ}\right) + \frac{1}{2}\frac{\partial^2}{\partial \phi^2}\left(\frac{H^2}{4\pi^2}P_{\rm HJ}\right) \tag{54}$$

$$\equiv -\frac{\partial J}{\partial \phi}, \tag{55}$$

to be solved with the boundary condition $P_{\rm HJ}(\phi_0, \alpha) = 0$, which implies that once a random walker ϕ among the ensemble ventures to $\phi = \phi_0$, it is removed—see, e.g., Ref. [48] for a detailed discussion of this boundary condition's use in exit problems.

H_0 (de Sitter) branch: Once the stochastically evolving field at a spatial point reaches ϕ_0, it is removed from the HJ branch and is injected into the degenerate $V = V_0$ (de Sitter) branch, where $H = H_0 = \sqrt{V_0/3}$. It then diffuses along the semi-infinite branch $\phi \in [\phi_e, \infty)$ of the flat potential $V = V_0$ according to the Langevin equation,

[4]We are therefore using a uniform expansion gauge in perturbation theory terminology. This is not fully equivalent to choosing spatially flat time slices but, as pointed out in Ref. [4], volume-preserving shape deformations are not interesting dynamically in our approximations. See also Appendix A on this point.

$$\frac{d\phi}{d\alpha}=\frac{H_0}{2\pi}\xi(\alpha), \tag{56}$$

again with

$$\langle\xi(\alpha)\xi(\alpha')\rangle=\delta(\alpha-\alpha'), \tag{57}$$

where now the influx from the HJ branch must also be accounted for. When the exit point ϕ_e of the $V=V_0$ branch is reached, inflation may end, for example, by entering a non-slow-roll region or by instant reheating, or the field may enter a subsequent slow-roll phase. In either case, the quantity of interest is the number of e-folds until ϕ_e is reached, which is a stochastic quantity.

We can write the probability distribution for ϕ on the H_0 branch as

$$P_{V_0}(\phi)=P_D(\phi)+P_\star\delta(\phi-\phi_0), \tag{58}$$

where P_D is the part which has diffused along the $V=V_0$ surface, while $P_\star$ denotes the probability at ϕ_0 leaking in from the HJ branch. Its contribution to the Fokker-Planck equation on the $V=V_0$ branch can be computed as follows: in a time interval between α and $\alpha+d\alpha$, the amount of random walkers flowing in from the HJ branch is

$$dP_\star=\int_{\phi_0}^{\infty}[P_{\rm HJ}(\phi,\alpha+d\alpha)-P_{\rm HJ}(\phi,\alpha)]d\phi. \tag{59}$$

Therefore,

$$\frac{\partial P_\star}{\partial\alpha}=\int_{\phi_0}^{\infty}\frac{\partial P_{\rm HJ}}{\partial\alpha}d\phi=J(\phi_0,\alpha), \tag{60}$$

and the Fokker-Planck equation for P_{V_0} can then be written as

$$\frac{\partial P_{V_0}}{\partial\alpha}=\frac{1}{2}\frac{\partial^2}{\partial\phi^2}\left(\frac{V_0}{12\pi^2}P_{V_0}\right)+J(\phi_0,\alpha)\delta(\phi-\phi_0), \tag{61}$$

where, recalling that $P_{\rm HJ}(\phi_0)=0$ and $\partial_\phi H(\phi_0)=0$,

$$J(\phi_0,\alpha)=\frac{V_0}{24\pi^2}\frac{\partial P_{\rm HJ}}{\partial\phi}\bigg|_{\phi_0}. \tag{62}$$

The probability distribution for the number of e-folds it takes for the field to reach ϕ_e can be obtained from knowledge of P_D by noting that once the random walker has been injected into the V_0 branch and has started diffusing, the probability that it has not yet crossed ϕ_e by the time of $\mathcal{N}$ e-folds is the same as that of inflation lasting longer than $\mathcal{N}$ e-folds:

$$\begin{aligned}\text{Prob(Inflationary duration} > \mathcal{N}) &= \int_{\mathcal{N}}^{\infty}\varrho(\alpha)d\alpha\\ &=\int_{\phi_e}^{\infty}P_D(\phi,\mathcal{N})d\phi,\end{aligned} \tag{63}$$

where we have denoted the probability that inflation lasts (more precisely, ϕ_e is reached) between α and $\alpha+d\alpha$ e-folds by $\varrho(\alpha)$. Therefore,

$$\varrho(\mathcal{N})=-\frac{\partial}{\partial\mathcal{N}}\int_{\phi_e}^{\infty}P_D(\phi,\mathcal{N})d\phi. \tag{64}$$

Using Eqs. (58), (60), and (61), we obtain simply

$$\varrho(\mathcal{N})=\frac{V_0}{24\pi^2}\frac{\partial P_{V_0}(\phi,\mathcal{N})}{\partial\phi}\bigg|_{\phi_e}. \tag{65}$$

A. Computing $P_{\rm HJ}$

In order to obtain the current flowing into the V_0 branch from Eq. (62), we first need to compute $P_{\rm HJ}$, the probability distribution on the HJ branch. To obtain simple analytic expressions, we will make the approximation that ϕ is close to ϕ_0 on the HJ branch, corresponding to a small initial velocity. This is justified, since

$$\phi_{\rm in}-\phi_0=\text{arc sinh}\left(-\frac{\Pi_{\rm in}}{\sqrt{2}V_0^{1/2}}\right)\simeq-\frac{\Pi_{\rm in}}{\sqrt{2}V_0^{1/2}}\ll 1, \tag{66}$$

assuming that the field enters the USR regime from a previous slow-roll phase. We will tackle the more general problem in an upcoming publication [40]. We therefore take the HJ branch stochastic dynamics to be [see Eq. (38)]

$$\frac{d\phi}{d\alpha}\simeq-3(\phi-\phi_0)+\frac{H_0}{2\pi}\xi(\alpha), \tag{67}$$

with exit boundary conditions at ϕ_0. Setting $\chi=\frac{\sqrt{12}\pi}{H_0}(\phi-\phi_0)$, the corresponding Fokker-Planck equation (54) for the probability density $P_{\rm HJ}(\chi,\alpha)$ reads

$$\frac{\partial P_{\rm HJ}}{\partial\alpha}\simeq 3\frac{\partial}{\partial\chi}(\chi P_{\rm HJ})+\frac{3}{2}\frac{\partial^2 P_{\rm HJ}}{\partial\chi^2}. \tag{68}$$

Writing

$$P_{\rm HJ}(\chi,\alpha)=Ce^{\frac{3}{2}\alpha-\frac{1}{2}\chi^2}\Psi(\chi,\alpha), \tag{69}$$

where C is a constant independent of α and χ but dependent on the choice of the initial state, $\Psi(\chi,\alpha)$ obeys

$$-\frac{1}{3}\frac{\partial\Psi}{\partial\alpha} = \frac{1}{2}\left(-\frac{\partial^2}{\partial\chi^2} + \chi^2\right)\Psi, \tag{70}$$

and the problem reduces to the quantum mechanical kernel for the *simple harmonic oscillator* (SHO), with a mass m and frequency ω given by $m\omega \to \hbar H_0^2/(12\pi^2)$ in imaginary time $\alpha = i\omega t/(3\hbar)$ (or $t = -3i\hbar\alpha/\omega$)—see, e.g., Ref. [51]. The free propagator, also known in the literature on stochastic processes as the *Mehler heat kernel* [52], is given by

$$K_M(\chi,\alpha;\chi_{\rm in},\alpha_{\rm in}) = \frac{1}{\sqrt{2\pi\sinh[3(\alpha-\alpha_{\rm in})]}}\exp\left(-\frac{\coth[3(\alpha-\alpha_{\rm in})](\chi^2+{\chi_{\rm in}}^2)}{2} + \frac{\chi\chi_{\rm in}}{\sinh[3(\alpha-\alpha_{\rm in})]}\right), \tag{71}$$

which for small time intervals tends to

$$\lim_{\alpha\to\alpha_{\rm in}} K_M(\chi,\alpha;\chi_{\rm in},\alpha_{\rm in}) = \delta(\chi-\chi_{\rm in}). \tag{72}$$

Since a random walker is "removed" upon reaching $\chi = 0$ ($\phi = \phi_0$), for the problem at hand we do not require the free, but rather the absorptive kernel. Due to the symmetry of the effective potential in which the dynamics takes place, it can be obtained from the full kernel [Eq. (71)] by adding to it a free *mirror* kernel at $-\chi$, giving

$$\begin{aligned}\Psi(\chi,\alpha) &= K_M(\chi,\alpha;\chi_{\rm in},\alpha_{\rm in}) - K_M(-\chi,\alpha;\chi_{\rm in},\alpha_{\rm in})\\ &= \sqrt{\frac{2}{\pi}}\frac{\exp\left(-\frac{1}{2}\coth[3(\alpha-\alpha_{\rm in})](\chi^2+{\chi_{\rm in}}^2)\right)}{\sqrt{\sinh[3(\alpha-\alpha_{\rm in})]}}\\ &\quad\times\sinh\left(\frac{\chi\chi_{\rm in}}{\sinh[3(\alpha-\alpha_{\rm in})]}\right),\end{aligned} \tag{73}$$

which ensures that the correct boundary condition is satisfied. The properly normalized $P_{\rm HJ}$ is then obtained from Eq. (69),

$$P_{\rm HJ}(\varphi,\alpha) = \frac{6\pi}{\sqrt{V_0}}\exp\left(\frac{3}{2}(\alpha-\alpha_{\rm in}) - \frac{1}{2}(\chi^2-\chi_{\rm in}^2)\right)\Psi(\chi,\alpha), \tag{74}$$

where C in Eq. (69) is chosen such that in the limit $\alpha\to\alpha_{\rm in}$ reduces to[5]

$$P_{\rm HJ}(\varphi,\alpha\to\alpha_{\rm in}) = \frac{6\pi}{\sqrt{V_0}}\delta(\chi-\chi_{\rm in}) = \delta(\phi-\phi_{\rm in}) \tag{75}$$

for ($\chi \geq 0, \chi_{\rm in} > 0$). A general probability distribution on the HJ branch can be obtained by convolving the absorptive kernel [Eq. (73)] with the initial probability distribution.

The injected current into the flat V_0 branch [Eq. (62)], $J = [\sqrt{V_0}/(4\pi)]\partial_\chi P_{\rm HJ}|_{\chi\to 0}$, is obtained by taking a derivative of Eq. (74):

$$J(\alpha) = \frac{6\pi}{[2\pi\sinh[3\Delta\alpha]]^{3/2}}\times\exp\left[\frac{3}{2}\Delta\alpha - \frac{1}{2}(\coth[3\Delta\alpha]-1)\chi_{\rm in}^2\right]\chi_{\rm in}, \tag{76}$$

which rises at early times $\Delta\alpha = \alpha - \alpha_{\rm in} \ll 1$ as

$$J(\alpha)|_{\Delta\alpha\ll 1} = \frac{\chi_{\rm in}}{\sqrt{6\pi}(\Delta\alpha)^{\frac{3}{2}}}e^{-\frac{\chi_{\rm in}^2}{6\Delta\alpha}}, \tag{77}$$

whereas at late times, when $\Delta\alpha = \alpha - \alpha_{\rm in} \gg 1$, it decays exponentially,

$$J(\alpha)|_{\Delta\alpha\gg 1} = \frac{6}{\sqrt{\pi}}\chi_{\rm in}e^{-3\Delta\alpha} + \mathcal{O}(e^{-9\Delta\alpha}). \tag{78}$$

The current $J(\alpha)$ for three different values of $\chi_{\rm in}$ can be seen in Fig. 2. The current increases from zero at $t = 0$

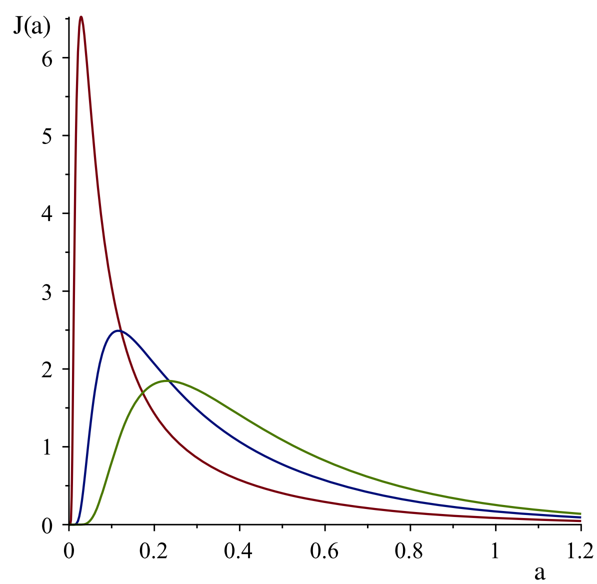

FIG. 2. The current $J(\alpha)$ injected from the HJ branch into the flat branch at $\phi = \phi_0$ for $\chi_{\rm in} = 0.5, 1, 1.5$ (from leftmost to rightmost curve).

[5]Strictly speaking, in the limit $\alpha\to\alpha_{\rm in}$, the probability density [Eq. (74)] reduces to $\delta(\chi-\chi_{\rm in}) + \delta(\chi+\chi_{\rm in})$. Since the domain of validity of Eq. (73) is the HJ branch on which $\chi \geq 0$, the second delta function is discarded.

($\alpha = \alpha_{\rm in}$), peaks, and then decays exponentially as $\propto e^{-3(\alpha-\alpha_{\rm in})}$—see Eqs. (77) and (78).

B. Computing $P_{\rm V_0}$

Assuming that the initial field distribution lies entirely at the HJ branch, Eq. (61) must be supplemented by the initial condition $P(\chi, 0) = 0$, and the solution can therefore be written as

$$P_{V_0}(\phi,\alpha) = \int_{\alpha_{\rm in}}^{\alpha} du\, G_{\rm e}(\phi-\phi_0, \alpha-u)J(u), \quad (79)$$

where $G_{\rm e}(\phi-\phi', \alpha-\alpha')$ is the diffusive Green function with exit boundary conditions at $\phi_{\rm e}$, also known as the absorptive kernel. As above, it is straightforwardly constructed from the well-known unrestricted diffusive kernel along an infinite interval

$$G(\phi,\phi',\Delta\alpha) = \sqrt{\frac{2\pi}{H_0^2\Delta\alpha}}\exp\left(-\frac{2\pi^2}{H_0^2\Delta\alpha}(\phi-\phi')^2\right), \quad (80)$$

where $\Delta\alpha = \alpha - \alpha'$, by subtracting the same kernel, but with ϕ' reflected on $\phi_{\rm e}$: $\phi \to 2\phi_{\rm e} - \phi$, giving

$$G_{\rm e}(\phi,\phi',\Delta\alpha) = \sqrt{\frac{2\pi}{H_0^2\Delta\alpha}}\left[\exp\left(-\frac{2\pi^2}{H_0^2\Delta\alpha}(\phi-\phi')^2\right) - \exp\left(-\frac{2\pi^2}{H_0^2\Delta\alpha}(2\phi_{\rm e}-\phi-\phi')^2\right)\right]. \quad (81)$$

This imposes the correct boundary conditions, $G_{\rm e}(\phi_{\rm e}, \phi', \Delta\alpha) = 0$ and $G_{\rm e}(\phi,\phi',\Delta\alpha\to 0) = \delta(\phi-\phi')$, for $\phi, \phi' \geq \phi_{\rm e}$. The limits of integration in Eq. (79) are determined by imposing that no current can be sourced before the beginning of inflation at $\alpha_{\rm in}$ (lower limit), and that no current can be sourced in the future of α (upper limit).

To compute the probability distribution for the field on the flat branch, we use the convolution integral [Eq. (79)] with the absorptive kernel [Eq. (81)] and the injected current [Eq. (76)] to obtain

$$P_{V_0}(\phi,\alpha) = \frac{3\chi_{\rm in}}{H_0}\int_0^\alpha \frac{du}{\sqrt{\alpha-u}}\left[\exp\left(-\frac{\chi^2}{6(\alpha-u)}\right) - \exp\left(-\frac{(\chi-2\chi_e)^2}{6(\alpha-u)}\right)\right] \times \frac{\exp\left[\frac{3}{2}u - \frac{1}{2}(\coth(3u)-1)\chi_{\rm in}^2\right]}{[\sinh(3u)]^{3/2}}, \quad (82)$$

where $\chi = \sqrt{12}\pi(\phi-\phi_0)/H_0$, $\chi_e = \sqrt{12}\pi(\phi_{\rm e}-\phi_0)/H_0$, and we set $\alpha_{\rm in} = 0$ for simplicity.[6]

C. Probability density for the *e*-fold number

From $P_{\rm V_0}$, we can directly compute the *e*-fold probability density using Eq. (65):

$$\varrho(\mathcal{N}) = \frac{\sqrt{3}}{2\pi}(-\chi_{\rm e}\chi_{\rm in}) \times \int_0^{\mathcal{N}} du \frac{\exp\left[-\frac{\chi_{\rm e}^2}{6(\mathcal{N}-u)} + \frac{3}{2}u - \frac{1}{2}(\coth(3u)-1)\chi_{\rm in}^2\right]}{[(\mathcal{N}-u)\sinh(3u)]^{3/2}}, \quad (83)$$

where we note that $\chi_{\rm e} < 0$ by definition. Although the above integrals cannot be evaluated analytically, an approximate evaluation of Eq. (82) can be performed by noting that the dominant dependence on u sits in the exponent, and the integral can be well approximated by a steepest descent method presented in Appendix B. There is a very simple case—namely, if the integral is dominated by $u \ll 1$, and if $\alpha \gg 1$, then it evaluates to

$$P_{V_0}(\phi,\alpha) \approx \frac{\sqrt{12}\pi}{H_0}\frac{e^{-\chi_{\rm in}^2/2}}{\sqrt{6\pi\Delta\alpha}} \times \left[\exp\left(-\frac{\chi^2}{6\Delta\alpha}\right) - \exp\left(-\frac{(\chi-2\chi_e)^2}{6\Delta\alpha}\right)\right], \quad (84)$$

which is, up to the factor $e^{-\chi_{\rm in}^2/2}$, equal to the absorptive kernel $G_e(\phi-\phi_0; \Delta\alpha)$ ($\Delta\alpha = \alpha - \alpha_{\rm in}$) in Eq. (81). Therefore,

$$\varrho(\mathcal{N}) \approx \sqrt{\frac{6}{\pi}} e^{-\frac{\chi_{\rm in}^2}{2}} \frac{e^{-\frac{\chi_{\rm e}^2}{6\mathcal{N}}}}{\mathcal{N}^{3/2}}. \quad (85)$$

We see that although $\varrho(\mathcal{N})$ is normalizable, the probability distribution does not decay fast enough, as $\phi \to \infty$, and therefore all moments are infinite: $\langle \mathcal{N}^n \rangle = \infty$ for $n \geq 1$. A numerical evaluation of the probability density $\varrho(\mathcal{N})$ is plotted in Fig. 3. For large $\mathcal{N}$, the distribution tends to an $\propto \mathcal{N}^{-3/2}$ decay, which is in agreement with our analytic estimate. This reflects the fact that if the precipice signified by $\phi_{\rm e}$ is beyond ϕ_0, the field settles into free diffusion along the half-line towards $\phi \to \infty$, a situation termed "infinite inflation" in Refs. [38,39].

The endless diffusion towards $\phi \to \infty$ would, of course, not occur if the field were injected into the de Sitter branch from a prior slow-roll regime. We will deal with this in

[6] One can always recover the dependence on $\alpha_{\rm in}$ by noting that the integral in Eq. (82) is a function of $\alpha - \alpha_{\rm in}$.

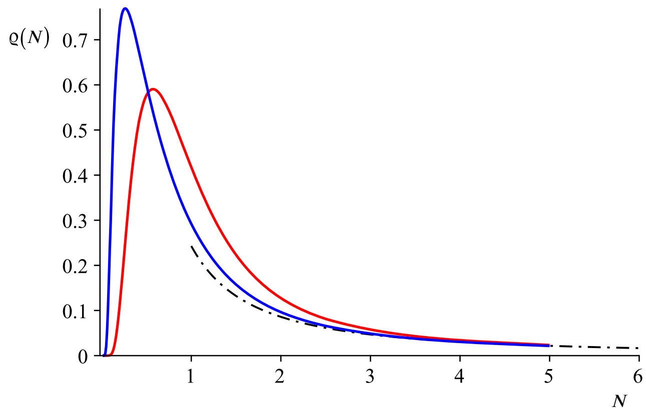

FIG. 3. The probability distribution $\varrho(\mathcal{N})$ defined by Eq. (83) for $\chi_e = -1$ and $\chi_{in} = 0.5$ (leftmost, blue curve) or $\chi_{in} = 1.5$ (rightmost, red curve). The dashed-dotted line indicates the asymptotic $\varrho \propto \mathcal{N}^{-3/2}$ behavior for large $\mathcal{N}$—see Eq. (85). This deep non-Gaussian tail is responsible for eternal inflation.

more detail in Ref. [40], where more complete models are studied. A simple way to regulate this infinite diffusion would be to erect a reflecting wall at, or close to ϕ_{in}. In Ref. [23], this is shown to indeed lead to a distribution with finite moments, and hence a finite curvature perturbation.

VI. THE CASE $\phi_e > \phi_0$: USR WITH GRACEFUL EXIT

We saw in the previous section that if the initial velocity of the field does not suffice to carry it beyond ϕ_e ($\phi_e < \phi_0$), eternal inflation sets in on the semiline $[\phi_e, \infty)$, and the curvature perturbation is infinite, as signified by the divergence of all moments of $\mathcal{N}$. We show in this section that this is not true when the exit point ϕ_e occurs on the HJ branch—i.e., before the asymptotic point $\phi = \phi_0$ at which the classical trajectory of ϕ would terminate. In other words, we now assume that

$$\phi_e \geq \phi_0 \tag{86}$$

and show that this model of inflation exhibits a graceful exit. The probability density $P_{HJ}(\phi, \alpha)$ is then of the form of Eq. (74), but with $\Psi(\chi, \alpha)$ given by the absorptive kernel mirrored at χ_e—see Eq. (73):

$$\begin{aligned}\Psi(\chi,\alpha) &= K_M(\chi,\alpha;\chi_{in},\alpha_{in}) - K_M(2\chi_e-\chi,\alpha;\chi_{in},\alpha_{in}) \\ &= \frac{1}{\sqrt{2\pi\sinh[3(\alpha-\alpha_{in})]}}\left\{\exp\left(-\frac{1}{2}\coth[3(\alpha-\alpha_{in})](\chi^2+\chi_{in}{}^2)+\frac{\chi\chi_{in}}{\sinh[3(\alpha-\alpha_{in})]}\right)\right. \\ &\quad \left. -\exp\left(-\frac{1}{2}\coth[3(\alpha-\alpha_{in})][(2\chi_e-\chi)^2+\chi_{in}{}^2]+\frac{(2\chi_e-\chi)\chi_{in}}{\sinh[3(\alpha-\alpha_{in})]}\right)\right\}. \end{aligned} \tag{87}$$

The probability $\varrho(\mathcal{N})$ in Eq. (64) that inflation ends in the interval $[\mathcal{N}, \mathcal{N}+d\mathcal{N})$ of e-folds is then

$$\varrho(\mathcal{N}) = -\frac{\partial}{\partial\mathcal{N}}\int_{\phi_e}^{\infty} d\phi P_{HJ}(\mathcal{N},\phi) \tag{88}$$

$$= -\frac{\partial}{\partial\mathcal{N}}\left\{\frac{1}{2}\mathrm{erfc}[\sqrt{1+n}(\chi_e - e^{-3\Delta\mathcal{N}}\chi_{in})] - \exp[\chi_{in}^2-\chi_e^2-(\chi_{in}-e^{-3\Delta\mathcal{N}}\chi_e)^2]\frac{1}{2}\mathrm{erfc}[\sqrt{n}(\chi_{in}-e^{-3\Delta\mathcal{N}}\chi_e)]\right\} \tag{89}$$

$$\begin{aligned} &= \frac{3\sqrt{n}}{\sqrt{\pi}}[2(1+n)\chi_{in} - (3+2n)e^{-3\Delta\mathcal{N}}\chi_e]\exp[-(1+n)(\chi_e - e^{-3\Delta\mathcal{N}}\chi_{in})^2] \\ &\quad - 3e^{-3\Delta\mathcal{N}}\chi_e[\chi_{in}-e^{-3\Delta\mathcal{N}}\chi_e]\mathrm{e}^{(\chi_{in}^2-\chi_e^2)-(\chi_{in}-e^{-3\Delta\mathcal{N}}\chi_e)^2}\mathrm{erfc}[\sqrt{n}(\chi_{in}-e^{-3\Delta\mathcal{N}}\chi_e)], \end{aligned} \tag{90}$$

where $n = 1/(e^{6\Delta\mathcal{N}}-1)$, $\Delta\mathcal{N} = \mathcal{N}-\mathcal{N}_{in}$, and $\mathrm{erfc}(z) = 1-\mathrm{erf}(z) = \frac{2}{\sqrt{\pi}}\int_z^\infty e^{-t^2}dt$ is the complementary error function. The distribution $\varrho(\mathcal{N})$ in Eqs. (88)–(90) is plotted in Fig. 4 for a few selected values of χ_e and χ_{in}. The distribution is again strongly non-Gaussian; however, at large $\mathcal{N}$ it falls off exponentially as $\propto \mathrm{e}^{-3\mathcal{N}}$, such that the moments of the curvature perturbation are all finite, implying that inflation terminates. The first term after the curly bracket in Eq. (89) is the standard result for the probability that the particle is located anywhere at $\chi > \chi_e$, and it approaches 1 when $\chi_e \to -\infty$, as it should, while the second term reduces the probability due to the absorptive boundary condition at $\phi = \phi_e$, where inflation ends.

Equations (88)–(90) contain the complete information for the probability distribution of the number of e-folds in this simple model [where we assume a small initial momentum, which allows us to linearize in $\phi - \phi_0$ in Eq. (67)]. To get a better understanding of $\rho(\mathcal{N})$ in

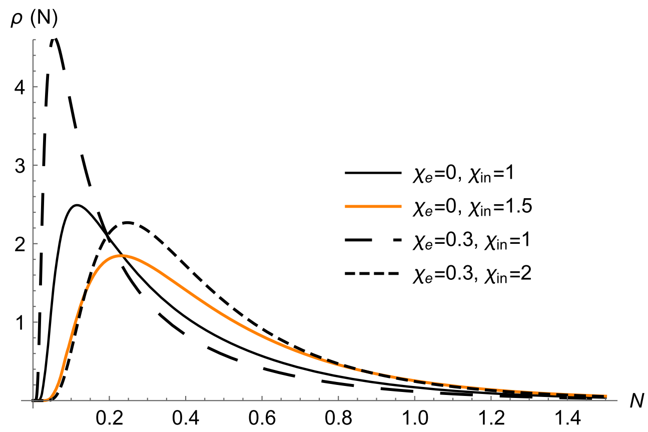

FIG. 4. The probability distribution [Eqs. (88)–(90)] in the USR model with graceful exit as a function of the number of e-folds, $\Delta\mathcal{N}=\mathcal{N}-\mathcal{N}_{\rm in}$ with $\mathcal{N}_{\rm in}=0$, and given in Eq. (90) for four choices of $(\chi_{\rm e},\chi_{\rm in})$: (0, 1) (solid black); (0, 1.5) (solid orange); (0.3, 1) (long dashes); and (0.3, 2) (short dashes). We see that for larger $\chi_{\rm e}$ ($\chi_{\rm in}$), inflation gets shorter (longer), which is as one would expect.

Eq. (88), we shall now calculate the first few moments of the number of e-folds:

$$\langle\mathcal{N}^k\rangle=\int_{\alpha_{\rm in}}^{\infty}\mathcal{N}^k\varrho(\mathcal{N})d\mathcal{N},\quad (k=0,1,2,\ldots).\tag{91}$$

Let us first look at the zeroth moment,

$$\langle 1\rangle=\frac{1}{2}[1+{\rm erf}[\chi_{\rm e}]+{\rm e}^{-\chi_{\rm e}^2}]\quad(\chi_{\rm e}\geq 0).\tag{92}$$

When $0\leq\chi_{\rm e}\lesssim 1$, this is, as one would expect, of the order 1. One can account for the fact that Eq. (92) is not exactly equal to 1 by dividing $\langle\mathcal{N}^n\rangle$ by $\langle 1\rangle$. The moments of $\mathcal{N}$ are considerably more difficult to calculate, and therefore in what follows, for simplicity we consider the case $\chi_{\rm e}=0$ ($\phi_{\rm e}=\phi_0$). Then the probability distribution in Eqs. (88)–(90) reduces to

$$\varrho(\mathcal{N})d\mathcal{N}=\frac{6\sqrt{n}}{\sqrt{\pi}}(1+n)\chi_{\rm in}{\rm e}^{-n\chi_{\rm in}^2}d\mathcal{N}.\tag{93}$$

It pays off to convert this into the probability per unit $dn=-6n(1+n)d\mathcal{N}$:

$$G(n)dn=\frac{\chi_{\rm in}}{\sqrt{\pi n}}{\rm e}^{-n\chi_{\rm in}^2}dn,\tag{94}$$

such that the kth moment in Eq. (91) gives

$$\langle\mathcal{N}^k\rangle=\frac{2}{\sqrt{\pi}}\int_0^{\infty}dy\,{\rm e}^{-y^2}\left[\frac{1}{6}\ln\left(1+\frac{\chi_{\rm in}^2}{y^2}\right)\right]^k,\tag{95}$$

where $(k=0,1,2,\ldots)$ and we use $y=\sqrt{n}\chi_{\rm in}$, assuming that $\alpha_{\rm in}=0$. Furthermore, it is useful to calculate how the number of e-folds fluctuates around its mean value, $\langle\mathcal{N}\rangle$:

$$\langle(\Delta\mathcal{N})^n\rangle=\sum_{k=0}^{n}(-1)^k\binom{n}{k}\langle\mathcal{N}^k\rangle\langle\mathcal{N}\rangle^{n-k},\tag{96}$$

where $\binom{n}{k}=n!/[k!(n-k)!]$ is the binomial coefficient.

The first moment in Eq. (96) can be expressed in terms of a generalized hypergeometric function,

$$\langle\mathcal{N}\rangle=\frac{\pi}{6}{\rm erf}(i\chi_{\rm in})-\frac{\chi_{\rm in}^2}{3}\times{}_2F_2\left(\{1,1\},\left\{\frac{3}{2},2\right\},\chi_{\rm in}^2\right).\tag{97}$$

The higher moments are harder to evaluate analytically. Nevertheless, one can show that the following confluent hypergeometric function generates all the moments:

$$\begin{aligned}\mathcal{G}(\alpha,\chi_{\rm in})&=\frac{2}{\sqrt{\pi}}\int_0^{\infty}dy\,{\rm e}^{-y^2}\left(1+\frac{\chi_{\rm in}^2}{y^2}\right)^{\frac{\alpha}{6}}\\&=\frac{1}{\sqrt{\pi}}\Gamma\left(\frac{1}{2}-\frac{\alpha}{6}\right)\times U\left(-\frac{\alpha}{6},\frac{1}{2},\chi_{\rm in}^2\right)\\&={}_1F_1\left(-\frac{\alpha}{6};\frac{1}{2};\chi_{\rm in}^2\right)-2\frac{\Gamma(\frac{1}{2}-\frac{\alpha}{6})}{\Gamma(-\frac{\alpha}{6})}(\chi_{\rm in}^2)^{1/2}\\&\quad\times{}_1F_1\left(\frac{1}{2}-\frac{\alpha}{6};\frac{3}{2};\chi_{\rm in}^2\right),\end{aligned}\tag{98}$$

in the sense that

$$\langle\mathcal{N}^k\rangle=\left(\frac{\partial^k}{\partial\alpha^k}\mathcal{G}(\alpha,\chi_{\rm in})\right)_{\alpha=0}(k=1,2,3,\ldots),\tag{99}$$

where U denotes the confluent hypergeometric function. In Fig. 5, we show the first few moments in Eq. (95) and their fluctuations around the mean $\langle\mathcal{N}\rangle$ defined in Eq. (96). For simplicity, we choose $\chi_{\rm e}=0$ and plot our results as a function of $\chi_{\rm in}$. We see that the distribution is highly non-Gaussian, which is one of the main results of this work. Because we have calculated $G(\alpha)$ with the assumption of small $\phi-\phi_0$, in Fig. 5 we plot the results only for $\chi_{\rm in}<1$. The principal conclusion is that the non-Gaussianities produced in USR are quite large and grow with $\chi_{\rm in}$, or the length of the USR supporting potential segment. On the other hand, from Fig. 4 we see that a larger $\chi_{\rm in}$ implies a larger average number of e-folds of USR $\langle\mathcal{N}\rangle$, from which we conclude that a longer USR phase generates larger non-Gaussianities. This observation can be of crucial importance for the generation of primordial black holes. These results are in broad agreement with the findings of Ref. [23], and it would be interesting to make a more quantitative comparison, recalling that we have fully and consistently included the gravitational effects of the field's velocity.

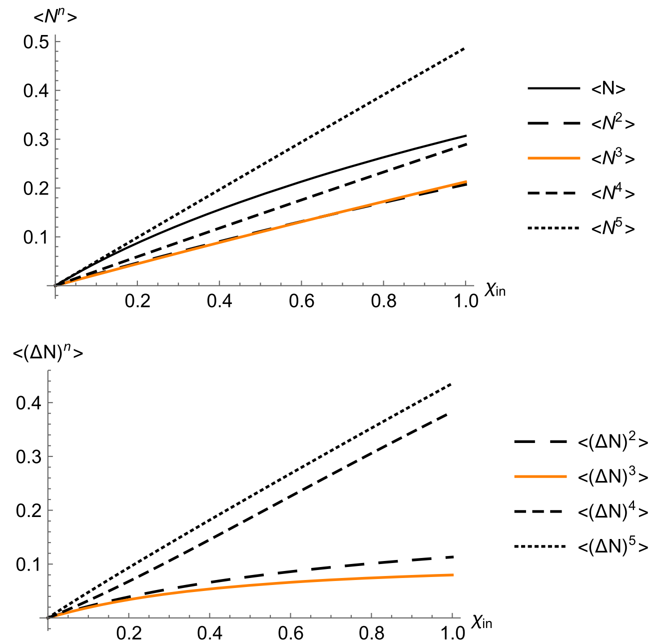

FIG. 5. The first few moments of the number of e-folds for $\chi_{\rm e} = 0$ as a function of $\chi_{\rm in}$ in our simple USR model. We show both the moments of $\mathcal{N}$ defined in Eqs. (91) and (95) (upper panel), as well as their fluctuation from the mean, $\langle(\Delta\mathcal{N})^n\rangle$, defined in Eq. (96) (lower panel).

VII. CONCLUSION AND DISCUSSION

In this paper, we established a consistent formalism for describing the quantum evolution of the large-scale curvature perturbation, generated during inflation on very flat portions of the potential $V(\phi)$, fully taking into account the scalar gravitational backreaction and the finite classical velocity for the field. This was achieved by combining a long-wavelength approximation to the Einstein equations with the stochastic picture of inflationary quantum fluctuations. We found that the $0i$ Einstein equation, usually neglected in the widely used "separate universe" approach, leads to a single stochastic equation for the scalar field but not its velocity, the latter being fully determined by the former even beyond slow roll through a unique solution to the Hamilton-Jacobi equation [Eq. (28)].

We then focused on a completely level potential $V = V_0$, where inflation occurs in an ultra slow-roll (USR) regime. We assumed that $\phi \in [\phi_{\rm e}, +\infty)$ and that the field is injected with some finite velocity $\Pi_{\rm in}$ at $\phi_{\rm in}$. We showed that on large (super-Hubble) scales, USR is a phase space attractor, in the sense that gravitational constraints fully fix the field velocity in terms of the field ϕ, up to a global constant ϕ_0 determined by the initial velocity and marking the end point towards which the classical field evolution asymptotes. This is accurate up to small, exponentially decaying gradient corrections, which are highly suppressed, and thus completely irrelevant on very large scales. The value $\phi_{\rm e}$ demarcates an exit point where inflation either ends or the field enters into another region of the potential, presumably one supporting slow roll. The stochastic number of e-folds required to reach $\phi_{\rm e}$ directly gives the curvature perturbation.

The inflaton dynamics depends crucially on the distance between the entry and exit points $|\phi_{\rm in} - \phi_{\rm e}|$ and on the initial field velocity $\Pi_{\rm in}$. As we argue in Sec. VI, if $|\phi_{\rm in} - \phi_0| > |\phi_{\rm in} - \phi_{\rm e}|$, the field performs a graceful exit, with $\phi_{\rm e}$ being eventually reached at all spatial points. If, on the other hand, $|\phi_{\rm in} - \phi_0| < |\phi_{\rm in} - \phi_{\rm e}|$, then the quantum phase space becomes larger than the classical one such that USR proceeds in two distinct phases, discussed in detail in Sec. V. When the quantum particle reaches the end point ϕ_0 of the classical trajectory, it will start diffusing along the set of classical trajectories marked by $\langle\Pi\rangle = 0$ and arbitrary ϕ, implying that the point ϕ_0 acts as a bifurcation point of the quantum phase space, at which the quantum trajectory splits into two branches—see Fig. 1. Consequently, a *conveyor belt* picture of the quantum particle phase space emerges and leads to a phase where some random walkers exit but most are trapped in an eternal de Sitter epoch as the field freely diffuses towards $\phi \to +\infty$. While in the former case, a well-defined probability distribution for the curvature perturbation emerges, in the latter, although normalizable, the distribution has no finite moments indicating an infinite curvature perturbation. This behavior, of course, depends on there not being a barrier in reaching $\phi \to +\infty$, a situation not valid in more complete inflationary models.

This is a preliminary study in many respects. In a realistic inflationary model, the flat potential portion will be finite, and even when $|\phi_{\rm in} - \phi_{\rm e}|$ is large and the conveyor belt is operational, the field's diffusion towards large values will be halted, although it may still lead to a greatly enhanced curvature perturbation. Furthermore, in passing to Eq. (67), we linearized in the field perturbation $\phi - \phi_0$, which is equivalent to assuming a small initial field velocity $\Pi_{\rm in}$. This was done for simplicity and to obtain the semianalytic results presented here but is not necessary. This paper was largely expository of the methods developed, and we will return with a more general treatment and more realistic USR models in a forthcoming publication [40]. Finally, we dropped the tensor modes which are nondynamical classically. This statement will no longer hold when their quantum fluctuations are taken into account. We reserve a more sophisticated nonlinear treatment of the IR stochastic tensors for the future.

ACKNOWLEDGMENTS

G. R. acknowledges partial supported by STFC Grant No. ST/P000371/1, Particles, Fields, and Spacetime. T. P. acknowledges the D-ITP consortium, a program of the NWO that is funded by the Dutch Ministry of Education, Culture, and Science (OCW). We would like to thank V. Vennin for very useful discussions and the anonymous referee for insightful comments that allowed us to clarify the approximations behind our computations.

APPENDIX A: CHANGING THE TIME-SLICING ON LONG WAVELENGTHS

In this Appendix, following Ref. [4], we recall that under changes of the time hypersurfaces $t \to T(t, \mathbf{x})$, the long-wavelength equations (17), (20), (21), and (22) remain invariant, and the long-wavelength spatial metric [Eq. (15)] retains its form. These statements are valid up to terms which are second order in spatial gradients and are therefore dropped within the long-wavelength approximation.

Starting with coordinates (t, x^i), consider a change in the choice of constant-time hypersurfaces (the spacetime time slicing) defined by a new time coordinate $T(t, x^i)$. To keep $N_i = 0$ in the new coordinate system, new spatial coordinates X^i must also be chosen which are orthogonal to the $T =$ const surfaces. We now examine how such a transformation between the old and new coordinates can be obtained.

Given the new time surface $T(t, x^i)$, a set of spatial coordinates X^i is chosen on a $T = T_0$ hypersurface and then orthogonally projected to thread all other $T =$ const hypersurfaces, labeling spatial coordinates in them too. Along constant X^i curves, the old coordinates x^μ will change as $dx^\mu = T^{,\mu} ds$, where s is an arbitrary parameter. Along such lines, T will change as

$$dT = T_{,\mu} dx^\mu = T_{,\mu} T^{,\mu} ds, \tag{A1}$$

which implies

$$\left(\frac{\partial x^\mu}{\partial T}\right)_{X^j} = \frac{T^{,\mu}}{T_{,\alpha} T^{,\alpha}}, \tag{A2}$$

which defines 4 of the 16 components of the transformation matrix between the old and new coordinates. To determine the 12 remaining components, we consider the transformation matrix

$$B_k^\mu = \left(\frac{\partial x^\mu}{\partial X^k}\right)_T, \tag{A3}$$

which should be chosen such that

$$T_{,\mu} B_k^\mu = 0 \tag{A4}$$

in order to keep $g_{TX^i} = 0$. If condition (A4) is satisfied on the $T = T_0$ hypersurface, it will always be satisfied. This can be seen by taking the T derivative of B_k^μ to find

$$\left(\frac{\partial B_k^\mu}{\partial T}\right)_{X^j} = \left(\frac{\partial}{\partial X^k}\left(\frac{\partial x^\mu}{\partial T}\right)_{X^j}\right)_T = \left(\frac{\partial}{\partial X^k}\left(\frac{T^{,\mu}}{T_{,\alpha} T^{,\alpha}}\right)\right)_T = B_k^\nu \left(\frac{T^{,\mu}}{T_{,\alpha} T^{,\alpha}}\right)_{,\nu}. \tag{A5}$$

In turn, this relation can be used to show that

$$\partial_T (T_{,\mu} B_k^\mu) = 0, \tag{A6}$$

and hence that N_i is kept at zero on all T time slices in the (T, X^j) coordinates.

From Eq. (A4), we have

$$B_k^0 = -\frac{B_k^i T_{,i}}{T_{,0}}, \tag{A7}$$

which, when substituted into Eq. (A5), gives

$$\left(\frac{\partial B_k^l}{\partial T}\right)_{X^j} = \left[\left(\frac{T^{,l}}{T^{,a} T_{,a}}\right)_{,m} - \frac{T_{,m}}{T_{,0}}\left(\frac{T^{,l}}{T^{,a} T_{,a}}\right)_{,0}\right] B_k^m. \tag{A8}$$

The rhs is second order in spatial gradients and is dropped within our approximation scheme, implying that to this order in the gradient expansion, B_k^l is independent of T:

$$B_k^l \equiv B_k^l(\mathbf{X}). \tag{A9}$$

On the other hand, by integrating x^j along a line of constant X^j using Eq. (A2), we obtain

$$x^j = f^j(\mathbf{X}) + \int \frac{T^{,j}}{T_{,0} T^{,0}} dT. \tag{A10}$$

This is consistent with Eq. (A9); a derivative of the second term with respect to X^j involves two spatial gradients $\partial/\partial x^i$, as can be seen by using Eq. (A7). Furthermore, any function evaluated at x^i will read

$$g(x^i) = g\left(f^i(\mathbf{X}) + \int \frac{T^{,j}}{T_{,0} T^{,0}} dT\right) \simeq g(f^i(\mathbf{X})) + g_{,i} \int \frac{T^{,j}}{T_{,0} T^{,0}} dT. \tag{A11}$$

Hence, within our approximations,

$$g(x^i) = g(f^i(\mathbf{X})) = \tilde{g}(X^i), \tag{A12}$$

and the 3-metric [Eq. (15)] in the $(T, \mathbf{x})$ coordinates reads

$$\gamma_{l'k'} = e^{2\alpha(t,\mathbf{x})} B^l_{l'}(\mathbf{X}) B^k_{k'}(\mathbf{X}) h_{lk}(\mathbf{x}) = e^{2\tilde{\alpha}(t(T),\mathbf{X})} B^l_{l'}(\mathbf{X}) B^k_{k'}(\mathbf{X}) h_{lk}(\mathbf{X}); \quad \text{(A13)}$$

i.e., it again has the form of a locally defined conformal factor times a time-independent 3-metric, which is only a function of the three new spatial coordinates X^i. The simplest choice for the new spatial coordinates is, of course, $f^j(\mathbf{X}) = X^j$.

Regarding the dynamical equations in the new time T, we note that for any time-dependent quantity Q,

$$\left(\frac{\partial Q}{\partial T}\right)_{X^j} = \frac{1}{T_{,0}}\left(\frac{\partial Q}{\partial t}\right)_{x^j} + \frac{T^{,k}}{T_{,0}T^{,0}}\left(\frac{\partial Q}{\partial x^k}\right)_t. \quad \text{(A14)}$$

Dropping the second term on the rhs as second order in spatial gradients, and noting that the two lapse functions, N_t and N_T, associated with the time coordinates t and T, respectively, are related by $N_t = N_T \partial T/\partial t$, we have

$$\frac{1}{N_T}\left(\frac{\partial Q}{\partial T}\right)_{X^j} = \frac{1}{N_t}\left(\frac{\partial Q}{\partial t}\right)_{x^j} \quad \text{(A15)}$$

up to second order in spatial gradients. This can be used to show the invariance of the long-wavelength dynamical equations under changes of the time slicing.

APPENDIX B: STEEPEST DESCENT FOR P_{V_0}

The integral in Eq. (82) is dominated by the dependence on u in the exponent, which diverges in both limits of integration, and hence is dominated by some intermediate u, at which the function in the exponent minimizes. To study the integral in more detail, we write it in the form

$$P_{V_0} = \frac{3\chi_{\rm in}}{H_0}[\mathcal{I}(\chi,\alpha) - \mathcal{I}(\chi - 2\chi_e,\alpha)], \quad \text{(B1)}$$

$$\mathcal{I}(\chi,\alpha) = \int_0^\alpha e^{-S(\chi,u)} du, \quad \text{(B2)}$$

where

$$S(\chi,u) = \frac{\chi^2}{6(\alpha-u)} + \frac{1}{2}\ln(\alpha-u) - 6u - \frac{3}{2}\ln(2) + n(6u)\chi^2_{\rm in} - \frac{3}{2}\ln[n(6u)], \quad \text{(B3)}$$

and where $n(x) = 1/(e^x - 1)$ is the Bose-Einstein function of its argument. The integral (B2) is then performed by expanding $S(\chi,u)$ in Eq. (B3) around the local minimum u_0 (at which $S'_0 \equiv [\partial_u S(\chi,u)]_{u=u_0} = 0$) as

$$S(u) \approx S(u_0) + \frac{1}{2}S''_0(u-u_0)^2 + \mathcal{O}((u-u_0)^3), \quad \text{(B4)}$$

where $S''_0 = [\partial_u^2 S(\chi,u)]_{u=u_0}$. Upon dropping the higher orders $\mathcal{O}((u-u_0)^3)$, the integral (B2) becomes simple to evaluate:

$$\mathcal{I}(\chi,\alpha) = \sqrt{\frac{\pi}{2S''_0}}\left[\mathrm{Erf}\left(\sqrt{\frac{S''_0}{2}}(\alpha-u_0)\right) + \mathrm{Erf}\left(\sqrt{\frac{S''_0}{2}}u_0\right)\right], \quad \text{(B5)}$$

where the result is meaningful if $S''_0 > 0$. To complete the evaluation, we need u_0 and S''_0, and hence we need the first and second derivatives of Eq. (B3):

$$S'_0 = \frac{\chi^2}{6(\alpha-u)^2} - \frac{1}{2(\alpha-u)} - 6n(n+1)\chi^2_{\rm in} + 3 + 9n = 0, \quad \text{(B6)}$$

$$S''_0 = \frac{\chi^2}{3(\alpha-u)^3} - \frac{1}{2(\alpha-u)^2} + 36n(n+1)(n+2)\chi^2_{\rm in} - 54n(n+1), \quad \text{(B7)}$$

where we make use of $\partial_u n(6u) = -6n(n+1)$ and $\partial_u^2 n(6u) = 36n(n+1)(n+2)$. u_0 is found by setting $S'_0 = 0$ in Eq. (B6). If $\alpha \gg u$, the problem of solving Eq. (B6) reduces to finding the positive root of a quadratic equation in $n = n(6u)$, which is easily solved for $n_0 \equiv n(6u_0)$, and hence also for u_0.

[1] S. W. Hawking, The development of irregularities in a single bubble inflationary universe, Phys. Lett. **115B**, 295 (1982).

[2] A. A. Starobinsky, Dynamics of phase transition in the new inflationary universe scenario and generation of perturbations, Phys. Lett. **117B**, 175 (1982).

[3] A. H. Guth and S. Y. Pi, The quantum mechanics of the scalar field in the new inflationary universe, Phys. Rev. D **32**, 1899 (1985).

[4] D. S. Salopek and J. R. Bond, Nonlinear evolution of long wavelength metric fluctuations in inflationary models, Phys. Rev. D **42**, 3936 (1990).

[5] M. Sasaki and E. D. Stewart, A general analytic formula for the spectral index of the density perturbations produced during inflation, Prog. Theor. Phys. **95**, 71 (1996).

[6] M. Sasaki and T. Tanaka, Superhorizon scale dynamics of multiscalar inflation, Prog. Theor. Phys. **99**, 763 (1998).

[7] D. H. Lyth, K. A. Malik, and M. Sasaki, A general proof of the conservation of the curvature perturbation, J. Cosmol. Astropart. Phys. 05 (2005) 004.
[8] D. H. Lyth and Y. Rodriguez, The Inflationary Prediction for Primordial Non-Gaussianity, Phys. Rev. Lett. **95**, 121302 (2005).
[9] N. S. Sugiyama, E. Komatsu, and T. Futamase, δN formalism, Phys. Rev. D **87**, 023530 (2013).
[10] J. Garriga, Y. Urakawa, and F. Vernizzi, δN formalism from superpotential and holography, J. Cosmol. Astropart. Phys. 02 (2016) 036.
[11] N. C. Tsamis and R. P. Woodard, Improved estimates of cosmological perturbations, Phys. Rev. D **69**, 084005 (2004).
[12] W. H. Kinney, Horizon crossing and inflation with large eta, Phys. Rev. D **72**, 023515 (2005).
[13] M. H. Namjoo, H. Firouzjahi, and M. Sasaki, Violation of non-Gaussianity consistency relation in a single field inflationary model, Europhys. Lett. **101**, 39001 (2013).
[14] J. Martin, H. Motohashi, and T. Suyama, Ultra slow-roll inflation and the non-Gaussianity consistency relation, Phys. Rev. D **87**, 023514 (2013).
[15] K. Dimopoulos, Ultra slow-roll inflation demystified, Phys. Lett. B **775**, 262 (2017).
[16] A. A. Starobinsky, Stochastic de Sitter (inflationary) stage in the early universe, Lect. Notes Phys. **246**, 107 (1986).
[17] D. S. Salopek and J. R. Bond, Stochastic inflation and nonlinear gravity, Phys. Rev. D **43**, 1005 (1991).
[18] K. Enqvist, S. Nurmi, D. Podolsky, and G. I. Rigopoulos, On the divergences of inflationary superhorizon perturbations, J. Cosmol. Astropart. Phys. 04 (2008) 025.
[19] T. Fujita, M. Kawasaki, Y. Tada, and T. Takesako, A new algorithm for calculating the curvature perturbations in stochastic inflation, J. Cosmol. Astropart. Phys. 12 (2013) 036.
[20] T. Fujita, M. Kawasaki, and Y. Tada, Non-perturbative approach for curvature perturbations in stochastic δN formalism, J. Cosmol. Astropart. Phys. 10 (2014) 030.
[21] V. Vennin and A. A. Starobinsky, Correlation functions in stochastic inflation, Eur. Phys. J. C **75**, 413 (2015).
[22] C. Germani and T. Prokopec, On primordial black holes from an inflection point, Phys. Dark Universe **18**, 6 (2017).
[23] C. Pattison, V. Vennin, H. Assadullahi, and D. Wands, Quantum diffusion during inflation and primordial black holes, J. Cosmol. Astropart. Phys. 10 (2017) 046.
[24] C. Pattison, V. Vennin, H. Assadullahi, and D. Wands, Stochastic inflation beyond slow roll, J. Cosmol. Astropart. Phys. 07 (2019) 031.
[25] M. Biagetti, G. Franciolini, A. Kehagias, and A. Riotto, Primordial black holes from inflation and quantum diffusion, J. Cosmol. Astropart. Phys. 07 (2018) 032.
[26] J. M. Ezquiaga and J. Garca-Bellido, Quantum diffusion beyond slow-roll: Implications for primordial black-hole production, J. Cosmol. Astropart. Phys. 08 (2018) 018.
[27] D. Cruces, C. Germani, and T. Prokopec, Failure of the stochastic approach to inflation beyond slow-roll, J. Cosmol. Astropart. Phys. 03 (2019) 048.
[28] H. Firouzjahi, A. Nassiri-Rad, and M. Noorbala, Stochastic ultra slow roll inflation, J. Cosmol. Astropart. Phys. 01 (2019) 040.
[29] S. Passaglia, W. Hu, and H. Motohashi, Primordial black holes and local non-Gaussianity in canonical inflation, Phys. Rev. D **99**, 043536 (2019).
[30] J. Garcia-Bellido, Primordial black holes, *Proc. Sci.*, EDSU2018 (2018) 042.
[31] N. C. Tsamis and R. P. Woodard, Stochastic quantum gravitational inflation, Nucl. Phys. **B724**, 295 (2005).
[32] F. Finelli, G. Marozzi, A. A. Starobinsky, G. P. Vacca, and G. Venturi, Generation of fluctuations during inflation: Comparison of stochastic and field-theoretic approaches, Phys. Rev. D **79**, 044007 (2009).
[33] F. Finelli, G. Marozzi, A. A. Starobinsky, G. P. Vacca, and G. Venturi, Stochastic growth of quantum fluctuations during slow-roll inflation, Phys. Rev. D **82**, 064020 (2010).
[34] B. Garbrecht, F. Gautier, G. Rigopoulos, and Y. Zhu, Feynman diagrams for stochastic inflation and quantum field theory in de Sitter space, Phys. Rev. D **91**, 063520 (2015).
[35] B. Garbrecht, G. Rigopoulos, and Y. Zhu, Infrared correlations in de Sitter space: Field theoretic versus stochastic approach, Phys. Rev. D **89**, 063506 (2014).
[36] I. Moss and G. Rigopoulos, Effective long wavelength scalar dynamics in de Sitter, J. Cosmol. Astropart. Phys. 05 (2017) 009.
[37] G. I. Rigopoulos, E. P. S. Shellard, and B. J. W. van Tent, Quantitative bispectra from multifield inflation, Phys. Rev. D **76**, 083512 (2007).
[38] H. Assadullahi, H. Firouzjahi, M. Noorbala, V. Vennin, and D. Wands, Multiple fields in stochastic inflation, J. Cosmol. Astropart. Phys. 06 (2016) 043.
[39] V. Vennin, H. Assadullahi, H. Firouzjahi, M. Noorbala, and D. Wands, Critical Number of Fields in Stochastic Inflation, Phys. Rev. Lett. **118**, 031301 (2017).
[40] G. Rigopoulos and A. Wilkins, Inflation is always semi-classical: Diffusion domination overproduces Primordial Black Holes, arXiv:2107.05317.
[41] G. I. Rigopoulos and E. P. S. Shellard, The separate universe approach and the evolution of nonlinear superhorizon cosmological perturbations, Phys. Rev. D **68**, 123518 (2003).
[42] P. Binetruy, E. Kiritsis, J. Mabillard, M. Pieroni, and C. Rosset, Universality classes for models of inflation, J. Cosmol. Astropart. Phys. 04 (2015) 033.
[43] A. R. Liddle, P. Parsons, and J. D. Barrow, Formalizing the slow roll approximation in inflation, Phys. Rev. D **50**, 7222 (1994).
[44] F. Cicciarella, J. Mabillard, and M. Pieroni, New perspectives on constant-roll inflation, J. Cosmol. Astropart. Phys. 01 (2018) 024.
[45] P. Friedrich and T. Prokopec, Entropy production in inflation from spectator loops, Phys. Rev. D **100**, 083505 (2019).
[46] P. H. Damgaard and H. Huffel, Stochastic quantization, Phys. Rep. **152**, 227 (1987).
[47] Bernt K. Oeksendal, *Stochastic Differential Equations: An Introduction with Applications* (Springer, Berlin, 2003), ISBN 3-540-04758-1; *Ludwig Arnold, Stochastic Differential Equations: Theory and Applications* (Wiley-Blackwell, New York, 1974), ISBN-10: 9780471033592, ISBN-13: 978-0471033592; I. I. Grihman and A. V.

Skorokod, *Stochastic Differential Equations* (Springer, New York, 1972); C. W. Gardiner, *Handbook of Stochastic Methods* (Springer-Verlag, Berlin, 2009), ISBN10 978-3-540-70712-7, ISBN13 978-3-642-08962-6.

[48] N. G. van Kampen, *Stochastic Processes in Physics and Chemistry*, 3rd ed. (North Holland, Amsterdam, 2007), ISBN 0-444-89349-0.

[49] T. Prokopec, N. C. Tsamis, and R. P. Woodard, Stochastic inflationary scalar electrodynamics, Ann. Phys. (Amsterdam) **323**, 1324 (2008).

[50] A. A. Starobinsky and J. Yokoyama, Equilibrium state of a self-interacting scalar field in the de Sitter background, Phys. Rev. D **50**, 6357 (1994).

[51] J. J. Sakurai and J. Napolitano, *Modern Quantum Mechanics*, 2nd ed. (Cambridge University Press, Cambridge, England, 2017).

[52] W. Pauli, *Wave Mechanics: Volume 5 of Pauli Lectures on Physics* (Dover Books on Physics, New York, 2000), ISBN 0486414620.